

Research Journal of Pharmaceutical, Biological and Chemical Sciences

Interfacially Synthesized Nanostructured Polyaniline Photocatalysts involving Phosphotungstic acid Doping and Poly (vinyl pyrrolidone) composite: Synergism and activity Enhancement in phenol degradation.

Rajesh Anantha Selvan P¹, Subramanian E^{2*}, and Murugesan R³

¹Department of Chemistry, St. John's College, Palayamkottai, Tirunelveli-627 002, Tamil Nadu, India.

²Department of Chemistry, Manonmaniam Sundaranar University, Tirunelveli-627 012, Tamil Nadu, India

³Department of Chemistry, TDMNS College, T. Kallikulam, Tirunelveli-627 113, Tamil Nadu, India

ABSTRACT

The present study has been undertaken to evaluate the photodegradation of phenol using PANI (polyaniline)/PTA (phosphotungstic acid)/PVP (Poly(vinyl pyrrolidone)) composite. Four catalysts PANI, PANI – PVP, PANI – PTA and PANI – PTA – PVP were synthesized by interfacial polymerization method (CCl₄ organic and aqueous acidic phases) and applied for photocatalysis. PTA doping with PANI or its PVP composite, as evident from SEM images, induced nanostructures (nanobristles/nanospheres) in the materials. Experiments at dark, under visible light and constant air flow were performed in order to assess the contribution of individual component. The effect of important parameters such as type of catalyst, phenol concentration, dose of catalyst, pH, volume of H₂O₂ and recycling of catalyst were also investigated. At the optimal condition of catalyst loading of 0.5 g/L of PANI-PTA-PVP, pH = 4, initial phenol concentration of 50 mg/L, constant air flow and H₂O₂ 2 ml maximum phenol degradation of 81.4 % in 160 min of irradiation time was achieved. The presence of synergic effect between PANI and PTA is believed to play the crucial role in enhancing the photoactivity. Thus, new composite, PANI-PTA-PVP emerged as the most efficient catalyst with the maintenance of activity even on repeated use.

Keywords: Polyaniline, Interfacial polymerization, Phosphotungstic acid dopant, Poly(vinyl pyrrolidone), Phenol photodegradation

**Corresponding author*

INTRODUCTION

Phenolic compounds are found to be one of the major hazardous materials that have a preilous impact on environment [1] and have significant impact to human health [2]. Exposure to these compounds can cause paralysis, anemia, liver damage and severe injury to the internal organs in human. The maximum permitted limit for phenol concentration in water by U. S. Environmental Protection Agency is 4 mg/L [3]. Different technological treatment methods are available for minimizing the concentration of phenols in aqueous solutions. These methods include chlorination [4], solvent extraction [5], membrane process [6], activated carbon adsorption [7], chemical oxidative degradation [8], biological digestion [9], etc. However, in each technique there are limitations and disadvantages [10].

The heterogeneous photocatalysis [11], is one of the advanced oxidation processes and solar/visible–light–driven photocatalysis is used for the degradation of phenol [12-15]. Photocatalysis field has attracted intense interest because of its low cost, high efficiency and lack of secondary pollution to the environment. Polyaniline (PANI) as a conducting polymer with an extended π -conjugated electron is a prominent photocatalyst due to its strong absorption in the visible–light and IR region and its high mobility of charge carriers. When light is irradiated, PANI not only is an electron donor but also an excellent hole acceptor. These special characteristics of PANI make this an ideal material to achieve enhanced charge separation efficiency in the photocatalysis. However, only a few studies have been reported on the combination of PANI and Heteropoly acid (HPA) to prepare composite photocatalyst [16,17] which can improve the photocatalytic performance.

Polyoxometalates are well-known catalysts for heterogeneous reactions [17]. Pure HPAs generally have low efficiency in catalytic reactions. HPAs are usually impregnated on polymers. There are two objectives in the present work: Doping of PANI with phosphotungstic acid (PTA), one of the polyoxometalates and HPAs and 2. an investigation of the resulting material for photocatalytic decomposition of phenol under visible region. Poly(vinyl pyrrolidone) (PVP) is a neutral polymer, which can function as a soft template [18]. Hence present investigation is targeted on the synthesis and material characteristics of interfacially polymerized PANI doped with/without PTA and loaded with/without structure-directing template, PVP. Four materials PANI, PANI-PVP, PANI-PTA and PANI-PTA-PVP were synthesized and applied as visible light photocatalysts.

EXPERIMENTAL

Materials

Aniline from Merck was distilled prior to use. Phosphotungstic acid was obtained from Sigma-Aldrich and used without further purification. CCl_4 , Con. HCl, PVP, N-methyl pyrrolidone (NMP), hydrogen peroxide and acetone were obtained from Merck. Sodium carbonate and Folin-phenol reagent were obtained from Spectrum Chemicals. Water was used after two distillations (DDW).

Synthesis of PANI materials

PANI was synthesized by interfacial polymerization using hydrogen peroxide as the oxidant [19]. In a typical procedure, 25 ml CCl_4 and 2 ml aniline were taken in a separatory funnel. Aqueous phase containing 2 ml H_2O_2 , 2 ml Con. HCl and 96 ml DDW was added gently to the organic phase. The aqueous phases in which PTA or PVP was added were sonicated initially (i.e, before polymerization). The reaction mixture (Fig. 1) was left undisturbed for four days for the completion of polymerization reaction. The polymer mass formed on fourth day was separated, washed several times with 0.1 M HCl, DDW and acetone until the washings became colourless. The samples were dried in an air oven at 110°C , ground into fine powder and stored in polythene packets. Similarly PANI - PVP and PANI – PTA were prepared by adopting the same procedure as above with 10 mM PVP or 5 mM PTA respectively. The sample PANI – PTA - PVP composite was also synthesized by adopting the same procedure as above with the same concentration of PVP and PTA.

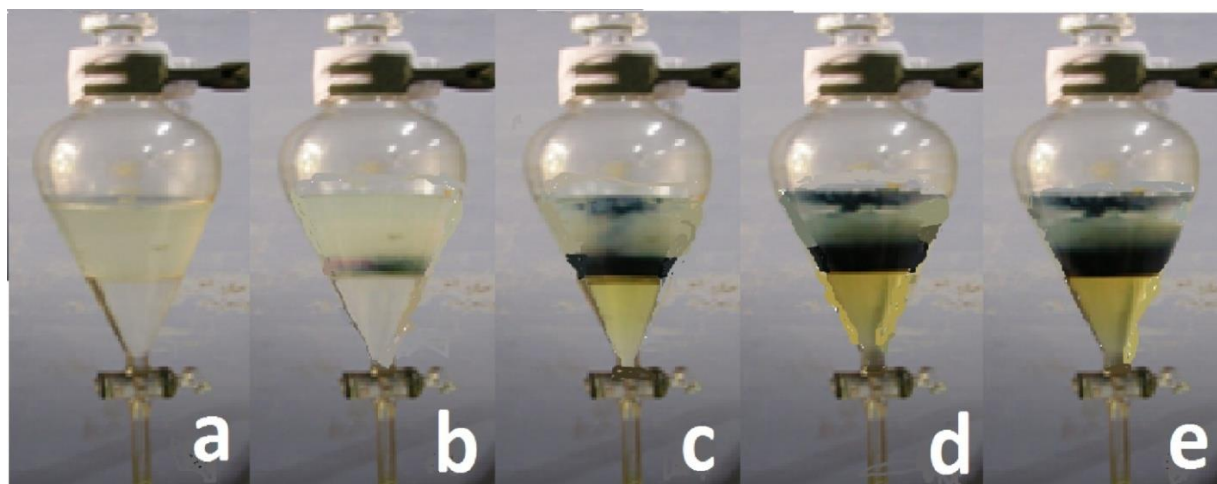


Fig. 1. Chemical oxidative Interfacial polymerization of PANI
 (a) 1 h (b) 4 h (c) 24 h (d) 48 h and (e) 96 h

Characterization

The UV-vis absorption spectra for PANI and its composites using NMP solvent were recorded with a Perkin Elmer UV-vis spectrophotometer (Lambda 25 model) in matched 1cm quartz cuvettes. FTIR spectra of all PANI materials in KBr pellet were recorded with JASCO FTIR - 410 spectrophotometer in the region 4000-400 cm^{-1} . Powder X-ray diffraction patterns of all PANI materials were obtained using a Shimadzu XRD 6000 X-ray diffractometer with Cu-K α radiation source ($\lambda = 1.54 \text{ \AA}$) operated at 40 kV and 30 mA in the 2θ range 10-90° at the scan speed of 10.0° per minute. Surface morphologies of all the powder samples were observed with JEOL JSM-6390 Scanning Electron Microscope (SEM) operating at 20 kV, after coating the samples with platinum for 45 s using JEOL JFC-1600 auto-fine coater with sputtering technique.

Photocatalysis

To analyse the photocatalytic behavior of PANI and its composite materials, Haber inner irradiation type photoreactor model HIPR-LC-150 with 150 W tungsten halogen lamp (light intensity = 14.79 mW/cm^2 at 555 nm measured with Kusem – Meco Luxmeter, model KM Lux 200 K) was used. The glass cylindrical flask was covered with aluminium foil during shaking and the course of reaction to avoid the fall of indoor light on reactor. A magnetic stirrer was used for through mixing of the photocatalyst with the phenol solution. A thermometer was inserted at the top of the photoreactor to measure temperature variations of the reaction. Phenol solution (300 ml) H_2O_2 (2 ml) and the required amount of the photocatalyst were fed into the photoreactor. The pH of the medium was adjusted by adding 0.1 M HCl or NaOH during the course of experiments. By using pump constant air was flown into the solution. All the experiments were carried out at atmospheric pressure and at the temperature of $28 \pm 2^\circ\text{C}$. Initially the phenol solution with the required quantity of catalyst was shaken for 30 min in the absence of light to reach adsorption/desorption equilibrium.

After equilibration, the first sample was taken to determine the initial concentration of phenol solution. After that tungsten lamp was switched on to start photocatalysis. 2 ml sample was drawn out for every 10 min for an hour and remaining samples were taken at 20 min intervals for a reaction time of 160 min. The samples were centrifuged and filtered using Whatman filter paper No. 1 to remove the suspended solids. Photodegradation study for the four catalysts PANI, PANI-PVP, PANI-PTA and PANI-PTA-PVP were carried out in light, constant air flow, H_2O_2 2 ml, at initial phenol concentration of 50 mg/L, pH 4 and dose of catalyst of 0.5 g/L. Experimental variables like initial phenol concentration, pH, dose of catalyst and reuse of catalyst were investigated. The percent of phenol degradation was analysed by using Phenol-Folin method [20]. In this method 2 ml phenol aliquot was mixed with 0.5 ml Phenol-Folin reagent and 2 ml sodium carbonate (20 % solution). This was diluted to 10 ml using DDW and the mixture was heated in a water bath for one minute to develop a blue colour. After 10 min of incubation, absorbance was measured at $\lambda_{\text{max}} = 650 \text{ nm}$. Phenol concentration of the sample was calculated using a standard graph. A series of known concentration of phenol was prepared and the absorbance was measured as described above. The standard graph was obtained by

plotting the absorbance vs concentration. The percent of photodegradation of phenol was calculated by using the equation (1).

$$\% \text{ Degradation} = (C_0 - C_t) 100 / C_0 \quad \text{----- (1)}$$

Where C_0 and C_t are the concentrations of phenol at initial and after irradiation time (t) respectively.

3. RESULTS AND DISCUSSION

UV-vis spectral studies

The UV-vis spectra of PANI and its composites in NMP solvent are displayed in Fig. 2 and the corresponding data in Table 1. In the literature, PANI has been shown with three absorption peaks at 325–360 nm, 390–410 nm and 575–620 nm [21-24]. In the present study, PANI shows three absorption bands at 335, 400 and 610 nm (Fig. 2a) assigned to π - π^* absorption of benzenoid rings and exciton absorption of the quinoid rings [21-23]. In NMP solvent, PANI – PVP exhibits the peak value of 331 nm, broad peak around 600 nm and a very broad band or tail at 1010 nm [24].

Table 1. UV-vis spectral and XRD data of PANI and its composites

Sample	UV-vis peaks in NMP solvent (nm)	XRD data		
		2 θ (deg)	d value (Å)	Average crystallite size (nm)
PANI	335, 400, 610	18.5	4.76	6.62
PANI-PVP	331, 600, 1010	27.1	3.11	5.56
PANI-PTA	350, 610, 985	28.3	1.68	9.24
PANI-PTA-PVP	350, 438, 600, 980	28.5	1.55	6.90

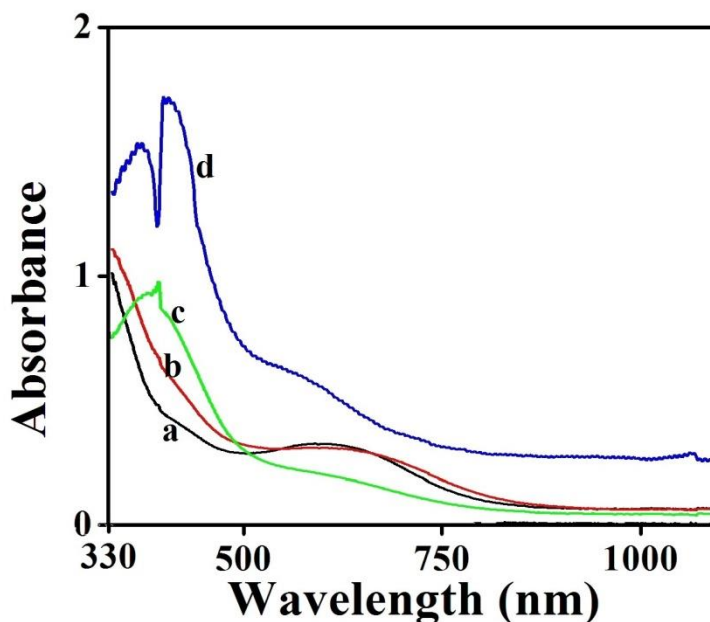


Fig. 2. UV-vis spectra of PANI and its composites in NMP solvent
(a) PANI (b) PANI-PVP (c) PANI-PTA and (d) PANI -PTA-PVP

In PANI – PTA the absorption peak below 350 nm, sharp absorption peak around 400 nm, broad peak at 610 nm and very broad peak or tail around 985 nm are observed. In literature, the spectral study of the PTA shows three absorption bands at 220, 260 and 310 nm due to the charge transfer (CT) transitions in the Keggin structure units [25,26]. Heteropoly acid (HPA), the non-reduced form is generally characterized by oxygen to

metal (O→M) charge transfer bands which appear in the UV region below 400 nm [25,26]. In PANI-PTA the charge transfer bands of PTA are mingled /merged with the π - π^* transition band of PANI. PANI – PTA – PVP exhibits strong peaks at 350 nm, 438 nm, broad peak around 600 nm and long wavelength tail around 980 nm. From reported study, absorption band below 350 nm of PANI – PTA - PVP is due to charge transfer transition in HPA [25-27]. PANI π - π^* peak around 400 nm is shifted to higher wavelength (438 nm) due to interaction with HPA. Absorption band around 600 nm and broad band around 980 nm are the characteristic absorptions of the doped states of PANI [27].

FTIR spectral studies

The FTIR spectra of PANI and its composites are shown in Fig. 3. The peaks values of PANI are 1578, 1500, 1402, 1291, 1175, 1064 and 803 cm^{-1} . The peaks at 1578 and 1500 cm^{-1} are due to stretching of quinoid ring (Q) and benzenoid ring (B) respectively [23-25,27-29]. The 1402 and 1291 cm^{-1} bands are due to C – N stretching vibration in QBQ, QBB and BBQ. A sharp peak at 1175 cm^{-1} , represents a mode of N=Q=N stretching vibration and a new peak at around 1064 cm^{-1} represents the C – N in plane bending mode of the ring. The C – H out-of-plane bending mode has been observed as a single band at 803 cm^{-1} [22,23,28].

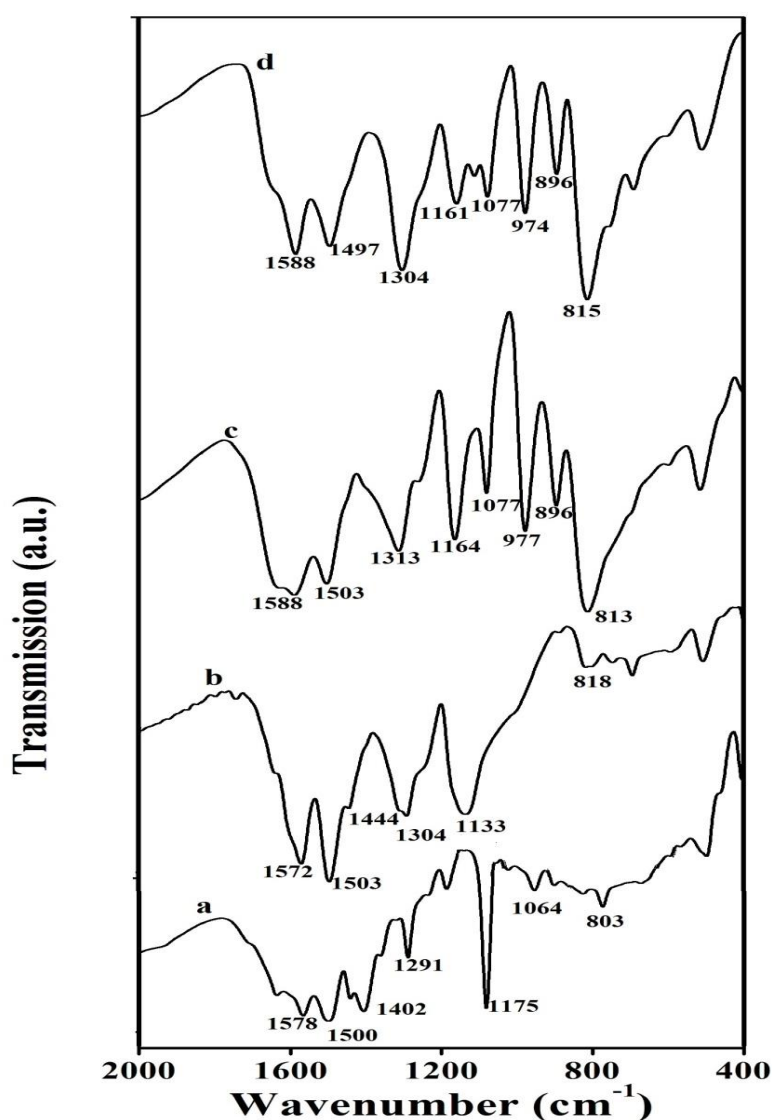


Fig. 3. FTIR spectra of (a) PANI, (b) PANI-PVP, (c) PANI-PTA and (d) PANI-PTA-PVP

The characteristic bands of PANI – PVP are at 1572, 1503, 1444, 1304, 1133 and 818 cm^{-1} . The characteristic vibrational bands of quinoid, benzenoid, C=N⁺ and C – N moieties and of dopant ions appear at

the usually observed positions reported in literature [22,23,28]. But the remarkable feature of the spectra is the explicit exposition of interaction of PVP with PANI in terms of shift, relative intensity change and splitting of the bands [29,30]. 1444 and 1304 cm^{-1} peaks are blue-shifted bands by the dopant ions. The three peaks of PANI at 950 - 1200 cm^{-1} are combined and appear as a single broad band at around 1133 cm^{-1} in PANI-PVP [29,30]. Further, peak at 803 cm^{-1} is shifted to 818 cm^{-1} in PANI - PVP. All these spectral features indicate strong interaction of PVP causing a chemical and structural change in PANI i.e, stretched/extended chain conformation of PANI by breaking intramolecular H- bonding [29,30].

For PANI-PTA peaks/bands occur at 1588, 1503, 1313, 1164, 1077, 977, 896 and 813 cm^{-1} with characteristic bands of PANI at 1588, 1503, 1313, 1164 and 813 cm^{-1} and that of PTA at 1077, 977, 896 and 813 cm^{-1} [25,31]. They confirm the presence of PANI and the PTA in the composite. IR spectra of PANI - PTA - PVP exhibit peaks at 1588, 1497, 1304, 1161, 1077, 974, 896 and 815 cm^{-1} . The positions of vibrational modes of all types of M-O bonds in PTA are heavily affected by the interaction with PANI. Some of the observations are below: W = O band of PTA in the composite is blue shifted from 968 cm^{-1} to 974 cm^{-1} and the band of W - O - W from 886 to 896 cm^{-1} [25,31]. The band of C-H out plane bending and W - O - W are blue shifted from 803 to 815 cm^{-1} . Thus IR spectral characterizations confirm the formation of PANI and its composites and also the interaction among its components.

XRD studies

XRD patterns of PANI and its composites are represented in Fig. 4 and the corresponding data from these patterns are given in Table 1. PANI shows two peaks, one at 18.5° and another at 24.9°. The patterns do not show sharp peaks and suggest amorphous nature to all the polymer samples except PANI-PTA-PVP (Fig. 4d). The XRD pattern of PANI is found to be matchable with the reported patterns of PANI [22,23,24,28].

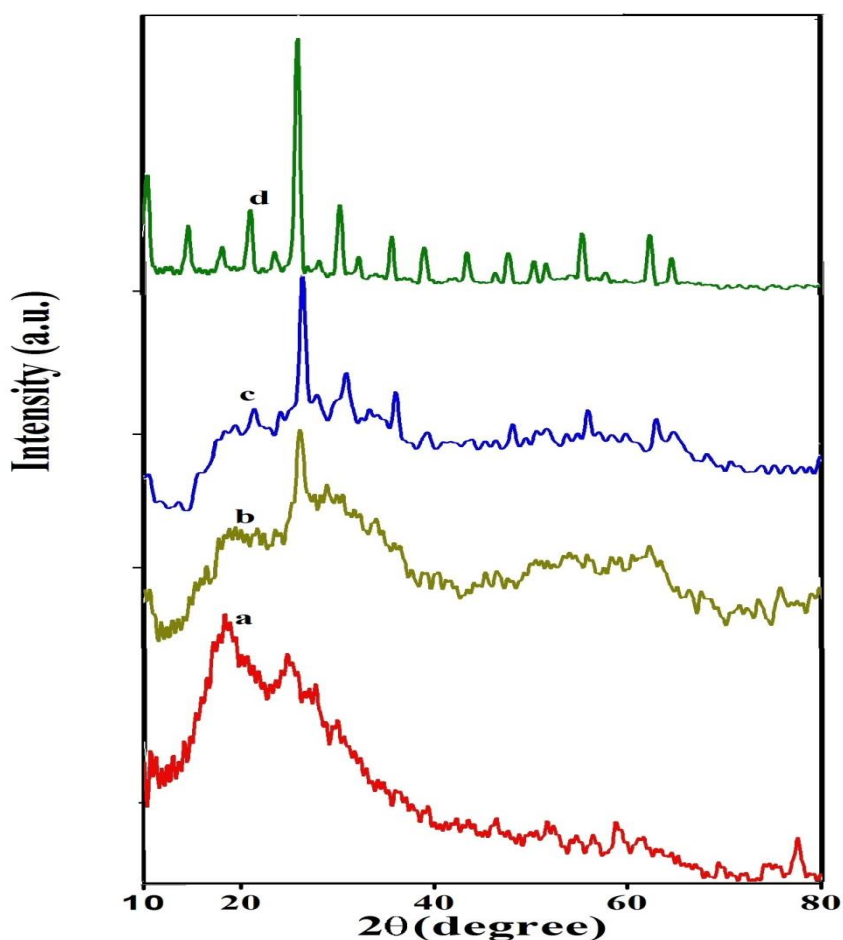


Fig. 4. XRD patterns of PANI materials (a) PANI, (b) PANI-PVP, (c) PANI- PTA and (d) PANI -PTA-PVP

Compared to PANI, PANI-PVP sample exhibits somewhat different XRD pattern. The lower peak of PANI at 18.5° has subdued while the higher angle peak at 24.9° has shifted to 27.1° . This shifting to higher angle side or lower d space with relatively sharp peak indicates the mutual interaction between PANI and PVP [24]. Larger size dopant PVP could establish a close contact with PANI chains and thereby enhance crystallinity [24].

PANI – PTA also exhibits a sharp signal at 28.3° with low d space together with low intense few other sharp signals at various positions. The lower angle signal at 18.5° is completely subdued. Appearance of sharp signals compared to the broad signals of PANI indicates improvement in crystallinity. This is substantiated further by the observation that PANI-PTA-PVP exhibits a pattern of completely sharp signals at various $2\theta/d$ values. The maximum intensity peak appears at 28.5° . This sharp multi-signal pattern indicates, beyond any doubt, the presence of crystallinity in PANI-PTA-PVP sample. The soft template PVP and the HPA -PTA mutually interact and also with PANI resulting in the conversion of amorphous PANI into a completely crystalline PANI-PTA-PVP sample. The average crystalline site values determined by Scherrer method are 6.62, 5.56, 9.24 and 6.90 nm for PANI, PANI-PVP, PANI-PTA and PANI–PTA–PVP samples respectively. The materials have nano-size particles. Thus XRD characterization not only proves the presence of each component but also their interaction and the amorphous/crystalline nature.

SEM studies

SEM images of PANI and its composites are shown in Fig. 5. PANI exhibits a morphology of almost spherically shaped, uniformly distributed and micron-sized particles/grains. These are all secondary particles/clusters consisting of nano-sized primary particles [32,33], which are all formed on agglomeration. One support for this observation is that even those secondary particles have surface-projected nano-size fringes/bristles – like structures which could be visualized on close view. Similar is the morphology with PANI-PTA sample (Fig. 5c) but such nanofringes are lesser in number. Similar nano-structured morphology is known in polymeric materials [34,35].

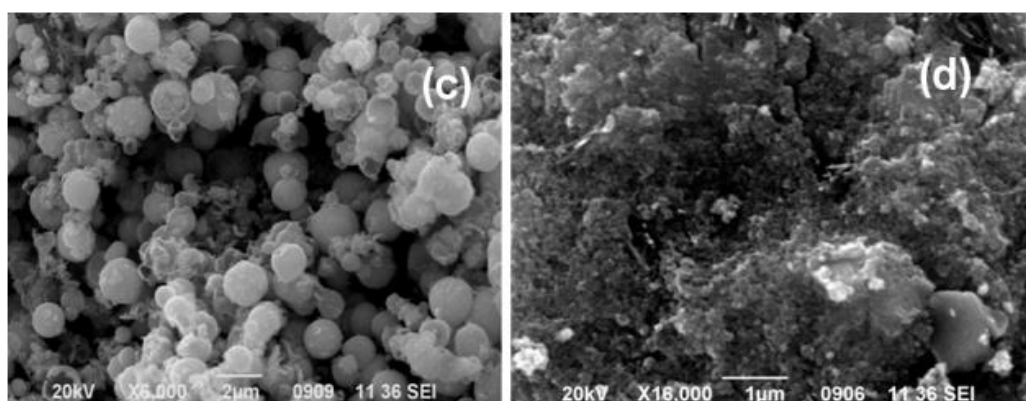


Fig. 5. SEM images of (a) PANI (b) PANI- PVP (c) PANI-PTA and (d) PANI-PTA-PVP

PANI-PVP and PANI-PTA-PVP (Fig.5b and d) on the other hand, have a different morphology. PANI-PVP has smooth-surfaced, random sized and non-uniformly shaped flakes. A strong agglomeration of primary spheres (randomly seen in Fig. 5b image) has resulted in such flakes. PANI-PTA-PVP has also flakes structures but here the flakes are of larger size, rough-surfaced and contain white dots/patches intensively distributed over all the entire flakes. By comparing PANI-PVP and PANI-PTA-PVP images (Fig. 5b and d), it is concludable that the PTA is present, perhaps, in the white dots/patches. The nano-fringes in PANI-PTA (Fig. 5c) are now present as embedded white dots/patches in flakes. The improvement in crystallinity of PANI-PTA and PANI-PTA-PVP, as observed from XRD (Fig. 5c and d) on addition of PTA to PANI or PANI-PVP, is reflected in SEM morphology as nano-fringes or nano-spheres or, in general, nano-crystalline structures [36,37].

Studies on Photodegradation

The preliminary experiments were carried out at conditions:1) PANI catalyst, under dark condition and air flow, 2) in light, constant air flow and H_2O_2 2 ml, (without catalyst); All the experiments were carried

out at initial phenol concentration of 50 mg/L, pH 4 and dose of catalyst of 0.5 g/L. The degradation of phenol at both the conditions (Fig. 6) is not significant [38] (3 % only was achieved). The photocatalytic activity of the four catalysts PANI, PANI-PVP, PANI-PTA and PANI-PTA-PVP under light, constant air flow; [phenol] = 50 mg/L; pH = 4; Temp: $28 \pm 2^\circ\text{C}$; and catalyst dose of 0.50 g/L (no H_2O_2) is represented by the % degradation of phenol by 4.6, 9.2, 21.5 and 46.4 % respectively (Fig. 7). All the components except H_2O_2 lead to decomposition of phenol. However, when 2 ml H_2O_2 was added to the above reaction system with PANI-PTA-PVP catalyst, 46.4 % degradation of phenol is almost doubled to 81.4 %. That means in addition to the above reaction components H_2O_2 is also essential which could boost the $\bullet\text{OH}$ radical formation and hence the phenol decomposition [39]. Hence, in all further experiments of optimization of experimental variables, H_2O_2 (2 ml) was added and they were proceeded. The results and their discussion succeed in following sections.

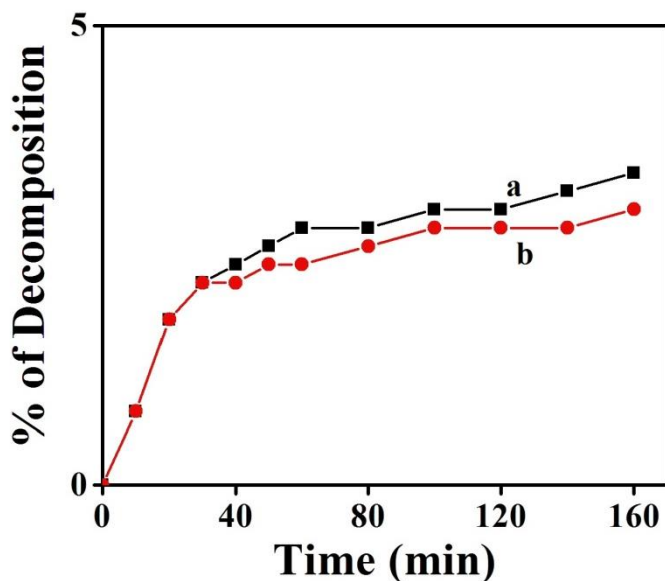


Fig. 6. Photocatalytic degradation of phenol (a) in dark in the presence of PANI and air flow (without oxidant H_2O_2) and (b) in light constant air flow and 2 ml H_2O_2 (without catalyst PANI)

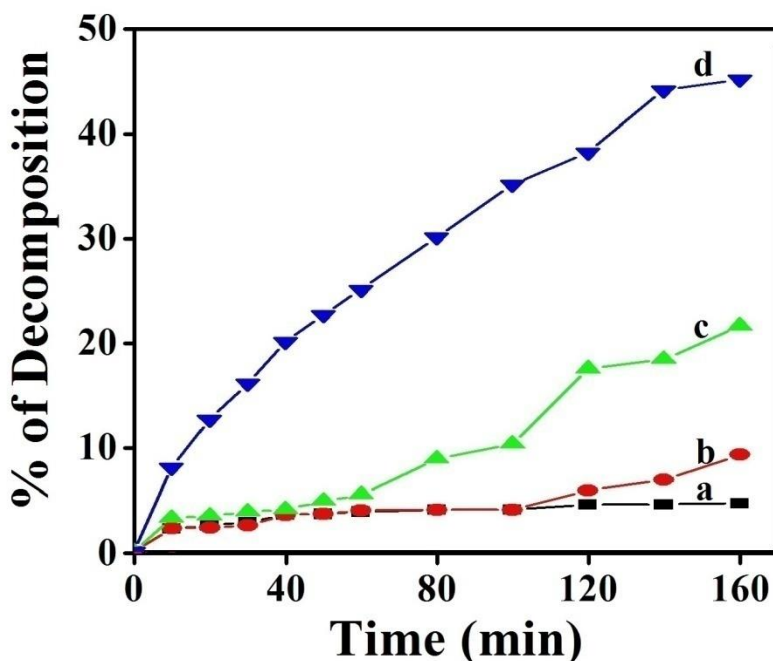


Fig. 7. Photocatalytic performance of (a) PANI (b) PANI- PVP (c) PANI-PTA and (d) PANI-PTA-PVP in phenol degradation Condition: [phenol] = 50 mg/L; pH = 4; Temp = $28 \pm 2^\circ\text{C}$; catalyst dose = 0.5 g/L and constant air flow (no H_2O_2).

Effect of types of catalyst with H₂O₂ and recycling of catalyst

The four different catalysts, PANI, PANI–PVP, PANI–PTA and PANI–PTA–PVP were subjected to visible light phenol degradation with H₂O₂ (2 ml), [phenol] = 50 mg/L; pH = 4; Temp = 28 ± 2°C and catalyst dose = 0.5 g/L and the results are displayed in Fig. 8. PANI–PTA–PVP shows maximum degradation (81.4 %) than PANI, PANI – PVP and PANI–PTA which exhibit phenol decomposition of 5.6, 15.4 and 59.2 % respectively. This result demonstrates clearly that the activity of PANI is increased by 3 times with PVP, while it is augmented more than 10 times by doping with PTA among this group. The activity increase of PANI with PTA doping is explained as follows. PTA is an electron acceptor [40,41] and can also function as electron-transfer agent. On visible light excitation of PANI, e⁻-h⁺ pair is formed. Conduction band electron, e⁻_{CB} of PANI is immediately accepted by PTA which then transfers to H₂O₂ so as to form radicals. By this way, the e⁻-h⁺ recombination, which is a significant factor in reducing the activity of photocatalyst, is avoided [40,41]. As a result, PANI–PTA is able to form more number of •OH radicals which, in turn, react with more number of phenol molecules and destruct them. Prevention of e⁻-h⁺ recombination is further facilitated by PVP and hence PANI–PTA–PVP catalyst could achieve greater efficiency. One point notable here is that there should be synergism between PTA and PANI in a constructive way, so that their combination and mutual interaction further enhances the efficiency of PANI–PTA (59.2 %) to 81.4 % in PANI–PTA–PVP.

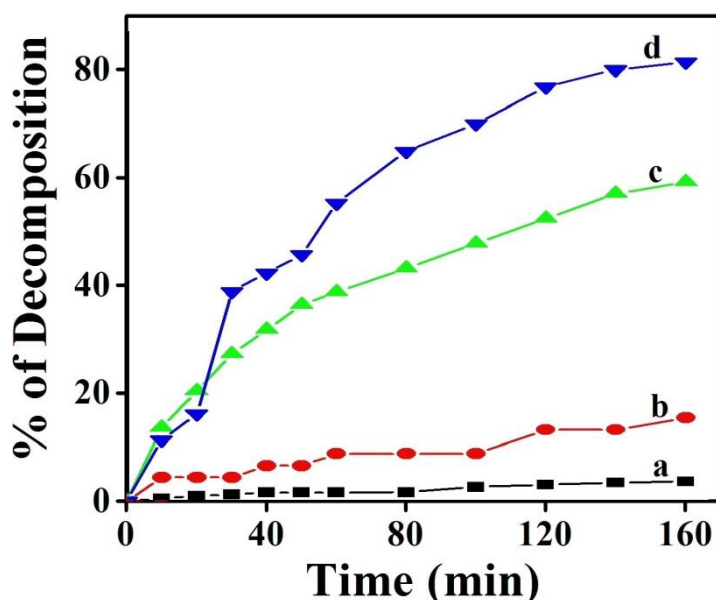


Fig. 8. Photocatalytic performance of (a) PANI (b) PANI- PVP (c) PANI-PTA and (d) PANI-PTA-PVP in phenol degradation
Condition: [phenol] = 50 mg/L; pH = 4; Temp: 28 ± 2°C; catalyst dose = 0.50 g/L, H₂O₂ = 2 ml and air flow.

The long term catalytic life of PANI–PTA–PVP was studied by repeated photocatalytic degradation under the same condition. Once the process was completed, the photocatalyst was recovered, washed with DDW, and dried in an oven without any further treatment. Second and third experimental cycles were run under the same conditions. The efficiency of the catalyst was reduced from 81.4 % to 64 %. This moderate decrease after 3 cycles may be due to incomplete removal of reaction intermediates [12].

Effect of initial phenol concentration

To assess the effect of initial phenol concentration on its degradation, the solutions with concentrations of 10, 30, 50 and 70 mg/L were fed to the reactor and the experiments were conducted. Results are shown in Fig. 9. When the initial phenol concentration was increased from 10 to 50 mg/L, the amount of degradation increased continuously; maximum degradation reached at 50 mg/L and then it decreased at 70 mg/L. With the increase in phenol concentration to 70 mg/L the available •OH radicals are inadequate for phenol degradation [42,43]. Hence 50 mg/L is the optimal phenol concentration.

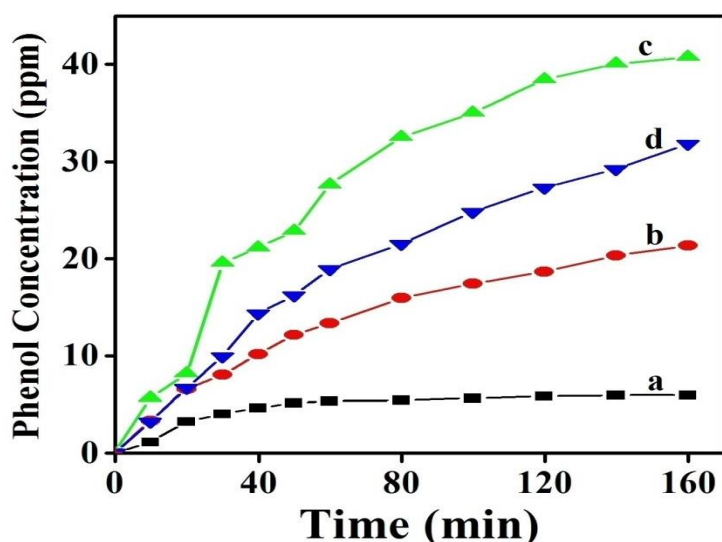


Fig. 9. Effect of initial phenol concentration on degradation (a) 10 mg/L (b) 30 mg/L (c) 50 mg/L and (d) 70 mg/L. Condition: pH = 4; Temp = $28 \pm 2^\circ\text{C}$; PANI-PTA-PVP dose = 0.50 g L^{-1} , $\text{H}_2\text{O}_2 = 2 \text{ ml}$ and air flow.

Effect of pH

The solution with optimal phenol concentration of 50 mg/L was considered for the experimental at the various pH values of 2, 4, 6, and 8 maintained by using 0.1 M HCl and NaOH. The percent of phenol removed was 46.6, 81.4, 58.8 and 15.8 % at pH 2, 4, 6 and 8 respectively (Fig. 10). This shows that phenol removal in aqueous solution by photocatalysis process depends on pH and pH 4 is optimal.

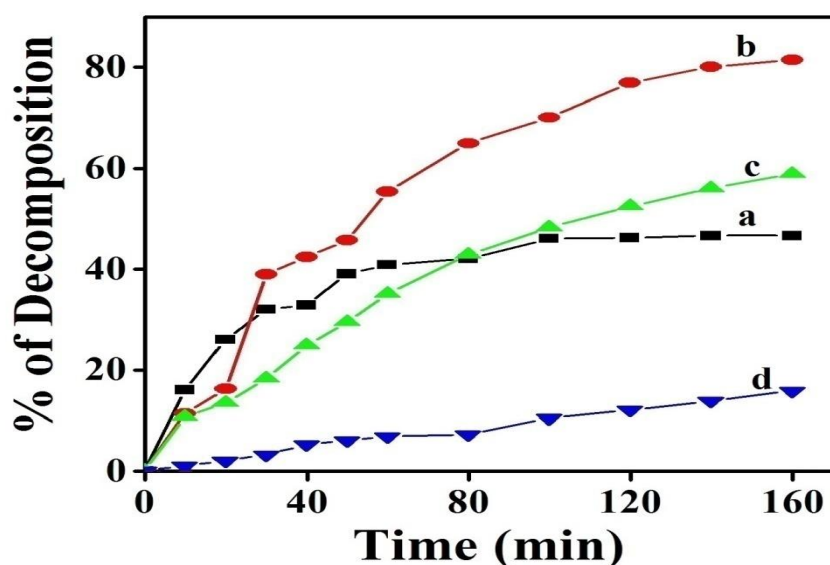


Fig. 10. Effect of pH on photodegradation of phenol (a) 2 (b) 4 (c) 6 and (d) 8. Condition: [phenol] = 50 mg/L; Temp = $28 \pm 2^\circ\text{C}$; PANI-PTA-PVP dose = 0.50 g/L , $\text{H}_2\text{O}_2 = 2 \text{ ml}$ and air flow

The point of zero charge, pH_{zpc} for PANI-PTA-PVP was determined as 6.95, an almost neutral pH. At highly acidic pH 2.0, the surface charge of the catalyst is positive, since H^+ can be attached to aniline group. This is an unfavorable situation. While at pH 8.0, the catalyst surface may be negative. Since pK_a of phenol is 11, at higher pHs 6 and 8, the proportion of availability of phenoxide ion will be increasingly higher. Hence there could be electrostatic repulsion between phenoxide and catalyst, which renders phenol adsorption difficult. Altogether pH 4.0 is a conducive condition for maximum adsorption of phenol and is, thus the optimal

pH condition. A similar observation has been noted in previous studies [44,45]. Thus at moderate pH value (pH = 4), phenol was degraded larger than at other pHs.

Effect of the dose of catalyst

In order to optimize the catalyst concentration, the effect of dosage on the degradation of phenol in aqueous solution was studied. The results are illustrated in Fig. 11. Phenol degradation increased with increase in dosage from 0.33 g/L and reaches a maximum of 81.4 % at a dosage of 0.50 g/L. However, increase in catalyst dosage to 0.66 g/L slightly reduces degradation % while dosage increase to 0.83 g/L has halved the % of degradation. The photocatalytic activity decreases at high value because of light scattering and screening effects. The tendency towards agglomeration (particle–particle interaction) also increases at high solids concentration [46,47]. Therefore 0.50 g/L is the optimal amount of photocatalyst for the degradation experiment.

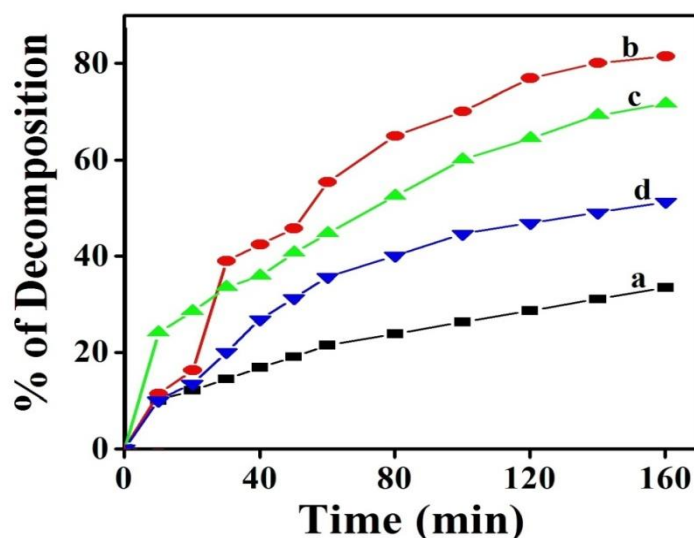


Fig. 11. Effect of catalyst dosage variation (g/L) on phenol degradation (a) 0.33 (b) 0.50 (c) 0.66 and (d) 0.83. Condition: pH = 4; [phenol] = 50 mg/L; Temp = 28 ± 2°C, H₂O₂ = 2 ml and air flow.

CONCLUSION

PANI, PANI–PVP, PANI–PTA and PANI–PTA–PVP materials were synthesized successfully by interfacial polymerization and characterized by UV-vis, FTIR, XRD and SEM techniques. XRD and SEM methods revealed the nano-features of the materials, particularly in PANI and PANI-PTA. SEM images showed the presence of nano-fringes over the surface of spherical particles. SEM also showed the presence of nano-spheres of PTA in the flakes of PANI-PTA-PVP. In photocatalysis, the preliminary experiments confirmed the essentiality of light, catalyst and O₂ for the degradation of phenol; otherwise the degradation extent was negligibly small. Even under this condition without H₂O₂, the catalyst exhibited only moderate efficiencies. In the presence of H₂O₂ only the efficiencies were significantly raised. The established optimal condition was pH = 4, H₂O₂ = 2 ml, catalyst dosage = 0.5 g/L, phenol concentration = 50 mg/L; under this condition, PANI-PTA-PVP exhibited the maximum efficiency (81.4 %). PTA augmented the efficiency of PANI through effective e⁻-h⁺ separation while the synergism between PTA and PVP improved the efficiency and ultimately PANI-PTA-PVP had the highest efficiency of all the four materials. On recycling and repeated use this catalyst maintained the efficiency. Altogether this study presents nano-structured PANI-PTA and PANI-PTA-PVP new catalysts synthesis by interfacial method and their greater efficiency in visible light degradation of the organic pollutant phenol.

REFERENCES

- [1] Leoufudi. I, Ziad. A, Amechrouq. A, Oukerrou. M. A, Mouse H. A, Mbarki. M., Identification and characterization of phenolic compounds extracted from Moroccan olive mill wastewater., *Food Sci. Technol, Campinas*, 2014, 34(2), 249-257.

- [2] Gad N. S, Saad. A. S., Effect of Environmental pollution by phenol on some physiological parameters of *Oreochromis niloticus*., *Global Veterinaria*, 2008, 2., 2(6), 312-319.
- [3] Hussain. A, Dubey. S. K, Kumar. V., Kintec study for aerobic treatment of phenolic wastewater., *Water Resources and Industry.*, 2015, 11, 81-90.
- [4] Britto-Costa. P. H, M. Ruotolo. L. A., Phenol removal from waste water by electrochemical oxidation using boron doped diamond (BDD) and Ti/Ti_{0.7}Ru_{0.3}O₂ DSA^R Electrodes., *Braz. J Chem. Eng.*, 2012, 29(04), 763-773.
- [5] Kujawski. W, Warszawski. A, Ratajczak. W, Porebski. T, Capala. W, Ostrowska. I., Removal of phenol from wastewater by different separation techniques., *Desalination.*, 2004, 163, 287-296.
- [6] Mnif. A, Tabassi. D, Ali. M. B. S, Hamrouni. B., Phenol removal from water by AG Reverse Osmosis Membrane., *Environ. Prog. Sustain.*, 2015, 1-8.
- [7] Dejene K, Siraj. K, Kitte. S. A., Kinetic and thermodynamic study of phenol removal from water using activated carbon synthesized from Avocado kernel seed., *Int. let. Nat. sci.*, 2010, 54, 42-57.
- [8] Kulkarni. S. J, Dr. Jayant, Kaware. P., Review on research for removal of phenol from wastewater., 2015, *IJSRP.*, 3(4), 1-5.
- [9] Tao. Y, Cheng. Z. L, Ting. K. E, Yin. X. J., Photocatalytic degradation of phenol using a nanocatalyst: The mechanism and kinetics., *J. Catal.*, 2013, A. ID: 364275, 1-6.
- [10] Rajemani. V, Reshma. J. K., Factors affecting phenol degradation potential of Microbes- A Review., *World J Pharm. Sci.*, 2016, 5(11), 691-706.
- [11] R. Rajeswari, S. Kanmani., TiO₂- Based heterogeneous photocatalytic treatment combined with oxonation for carbendazim degradation., *Iran. J. Environ. Health Sci. Eng.*, 2009, 6(2), 61-66.
- [12] Yawalkar. A. A, Bhatkhande. D. S, Pangarkar. V. G, Beenackers. M., Solar-assisted photochemical and photocatalytic degradation of phenol., *J. Chem. Technol. Biotechnol.*, 2001, 76, 363-370.
- [13] Qie. R, Zhang. D, Diao Z, Huang. X, He. C, Xiong. Y., Visible light induced photocatalytic reduction of Cr(VI) over polymer-sensitized TiO₂ and its synergism with phenol oxidation., *Water Res.*, 2012, 46, 2299-2306.
- [14] Thirumalairjan. S, Girija. K, Mastelaro. V.R, Ponpandian. N., Photocatalytic degradation of organic dyes under visible light irradiation by floral-like LaFeO₃ nanostructures comprised of nanosheet petals., *New J. Chem.*, 2014, 38, 5480-5490.
- [15] Rajeshwar. K, Chenthamarakshan. C. R, Goeringer. S, Djukic. M., Titania-based heterogeneous photocatalysis. Materials, mechanistic issues, and implications for environmental remediation., *Pure Appl. Chem.*, 2001, 73(12), 1849-1860.
- [16] Cui. S, Park. S., Electrochemistry of conductive polymers XXIII: polyaniline growth studied by electrochemical quartz crystal microbalance measurements., *Synth. Met.*, 1999, 105, 91-98.
- [17] Ren. Y, Wang. M, Chen. X, Yue. B, He. H., Heterogeneous catalysis of Polyoxometalate based Organic-Inorganic Hybrids., *Materials.*, 2015, 8, 1545-1567.
- [18] Li. C, Zhang. X, Wang. K, Zhang. H, Sun. X, Ma. Y., Dandelion-like cobalt hydroxide nanostructures: morphological evolution, soft template effect and supercapacitive application., *RSC Adv.*, 2014, 4, 59603-59613.
- [19] Zhu. J, Chen. M, Qu. H, Zhang. X, Wei. H, Luo. Z, Henry A. Colorado, Wei. S, Guo. Z., Interfacial polymerized polyaniline/graphite oxide nanocomposites toward electrochemical energy storage., *Polymer.*, 2012, 53, 5953-5964.
- [20] Lowry. O. H, Rosebrough. N. J, Farr. A. L, Randall. R. J., Protein measurement with the Folin Phenol Reagent., *J. Biol. Chem.*, 1951, 193, 265-275.
- [21] Ram. M. S, Palaniappan. S., A process for the preparation of polyaniline salt doped with acid and surfactant groups using benzoyl peroxide., *J. Mater. Sci.*, 2004, 39, 3069-3077.
- [22] Pruneanu. S, Veres. E, Marian. I, Oniciu. L., Characterization of polyaniline by cyclic voltammetry and UV-Vis absorption spectroscopy., *J. Mater. Sci.*, 1999, 34, 2733-2739.
- [23] Murugesan. R, Subramanian. E., The effect of Cu(II) coordination on the structure and electric properties of polyaniline-poly(vinyl alcohol) blend., *Mater. Chem. Phys.*, 2002, 77, 860-867.
- [24] Subramanian. E, Anitha. G, Vijayakumar. N, Constructive modification of conducting polyaniline characteristics in unusual proportion through nanomaterial blend formation with the neutral polymer Poly(vinyl pyrrolidone)., *J. Appl. Polym. Sci.*, 2007, 106, 763-683.
- [25] Gu. D, Liu. G, Wu. J, Shen. L., Synthesis of H₃PW₁₂O₄₀-H₂O- doped polyaniline by chemical oxidative polymerization., *Procedia Eng.*, 2012, 27, 1448-1453.
- [26] Rajkumar. T, Rao. G. R., Investigation of hybrid molecular material prepared by ionic liquid and polyoxometalate anion., *J. Chem. Sci.*, 2008, 120(6), 587-594.

- [27] Posudievsky. O.Y, Kurys. Y.I, Pokhodenko. V.D., 12-Phosphormolybdic acid doped polyaniline-V₂O₅ composite., *Synth. Met.*, 2004, 114, 107-111.
- [28] Chi. M. S, Kim. J. W, Choi. H. J, Webber. R. M, Jhon. M. S., Electrorheological characteristics of polyaniline and its copolymer suspensions with ionic and nonionic substituents., *Colloid Polym Sci.*, 2000, 278, 61-64.
- [29] Subramanian. E, Ramalakshmi. R. D, Vijayakumar. N, Sivakumar. G., Hybrid composite materials of anatase titania and conducting polyaniline: properties and chemical sensor application, *Indian J. Eng. Mater. Sci.*, 2012, 19, 237-244.
- [30] Vijayakumar. N, Subramanian. E, Padiyan. D. P., Cross-Linked Poly(vinyl pyrrolidone) Hard-template and polymerization method in controlling nanostructures and properties of polyaniline composites., *Poly Plast Technol.*, 2013, 52, 1220-1227.
- [31] Almedia. L.C.P, Goncalves. A.D, Benedetti. J.E, Miranda. P.C.M.L, Passoni. L.C, Nogueira. A.F., Preparation of conducting polyanilines doped with Keggin-type polyoxometalates and their application as counter electrode in dye-sensitized solar cells., *J. Mater. Sci.*, 2010, 45, 5054-5060.
- [32] Wang. H, Wen. H, Hu. B, Fei. G, Shen. Y, Sun. L, Yang. D., Facile approach to fabricate waterborne polyaniline nanocomposites with environmental benignity and high physical properties., *Sci. Rep.*, 2017, 7:43694, 1-12.
- [33] Zhang. X, Zhu. J, Haldolaarachchige. N, Ryu. J, Young. David P, Wei. S, Guo. Z., Synthetic process engineered polyaniline nanostructures with tunable morphology and physical properties., *Polymer.*, 2012, 53, 2109-2120.
- [34] Mostafaei. A, Zolriasatein. A., Synthesis and characterization of conducting polyaniline nanocomposites containing ZnO nanorods., *Prog. Nat. Sci.*, 2012, 22(4), 273-280.
- [35] Ma. Hui-yan, Luo. Yun-qing, Yang. Sheng-xue, Li. Yun-wu, Cao. F, Ging. J., Synthesis of Aligned polyaniline Belts by Interfacial control approach., *J. Phys. Chem. C.*, 2011, 115, 12048-12053.
- [36] Xu. J, Wang. K, Zu. Sheng-Zhen, Han. Bao-Hang, Wei. Z., Hierarchical Nanocomposites of polyaniline nanowire arrays on Graphene oxide sheets with Synergistic effect for Energy storage., *ACS NANO.*, 2010, 4(9), 5019-5026.
- [37] Michira. I, Akinyeye. R, Somerset. V, Klink. M. J, Sekota. M, Al-Ahmed. A., Synthesis, Characterisation of novel polyaniline Nanomaterials and application in Amperometric Biosensors., *Macromol. Symp.*, 2007, 255, 57-69.
- [38] Lin. Y, Li. D, Hu. J, Xiao. G, Wang. J, Li. W, Fu. X., Highly efficient photocatalytic degradation of organic pollutants by PANI-Modified TiO₂ composite., *J. Phys. Chem. C.*, 2012, 116, 5764-5772.
- [39] Laura G.C. Villegas, N. Mashhadi, M. Chen, D. Mukherjee, Keith E. Taylor, N. Biswas., A short review of techniques for phenol removal from Wastewater., *Curr. Pollution Rep.*, 2016, 2, 157-167.
- [40] Anandan. S, Yoon. M, Park. S., Photocatalytic effects of heteropolytungstic acid-encapsulated TiSBA-15 on decomposition of phenol in water., *J. Photo Sci.*, 2003, 10(3), 231-236.
- [41] Qie. R., Zhang. D, Diao. Z, Huang. X, He. C, Xiong. Y., Visible light induced photocatalytic reduction of Cr(VI) over polymer-sensitized TiO₂ and its synergism with phenol oxidation., *Water Res.*, 2012, 46, 2299-2306.
- [42] Lee. S, Oh. J, Rark. Y., Degradation of phenol with Fenton-like treatment by using Heterogeneous catalyst (Modified Iron Oxide) and Hydrogen Peroxide., *Bull. Korean Chem. Soc.*, 2006, 27(4), 489-494.
- [43] Gomez. H, Orellana. F, Lizama. H, Mansilla. D, Dalcliviele. E. A., Study of phenol Photodegradation with TiO₂/-WO₃ coupled semiconductors activated by visible light., *J. Chil. Chem. Soc.*, 2006, 51(4), 1006-1009.
- [44] Bazaga-Garcia. M, Cabeza. A, Olivera-Pastor. P, Santacruz. I, Colodrero. R. M. P, Aranda. M. A. G., 2012, "Photodegradation of Phenol over a Hybrid Organo-Inorganic Material: Iron(II) Hydroxyphosphonoacetate", *J. Phys. Chem. C.*, 116, 14526-14533.
- [45] Cruz. R, Reyes. L. H, Guzman-Mar. Jorge L, Peralta-Hernandez. J. M, Hernandez-Ramirez. A., "Photocatalytic degradation of phenolic compounds contained in the effluent of a dye manufacturing industry", *Sustain Environ. Res.*, 2011, 21(5), 307-312.
- [46] Gnanaprakasam. A, Sivakumar. V. M, Thirumarimurugan. M., Influencing parameters in the photocatalytic degradation of organic effluent via Nanometal oxide catalyst: A review., *Indian J Eng Mater S.*, 2015, ID: 601827, 1-16.
- [47] Fufa. T. O, Mengesha. A. T, Yadav. O. P., Photocatalytic activity of nanopolyaniline(NPA) on phenol degradation., *Afr. J. Pure Appl. Chem.*, 2016, 10(3), 33-41.